Original Article

Dynamic contrast-enhanced MRI of nasopharyngeal carcinoma: correlation of quantitative dynamic contrast-enhanced magnetic resonance imaging (DCE-MRI) parameters with hypoxia-inducible factor 1α expression and tumor grade/stage

Lan Liu[1,2], Liping Hu[1,2], Qiao Zeng[1,2], Dexin Peng[1,3], Zhiping Chen[1,4], Chuansheng Huang[1,5], Zhiliang Liu[1,5], Qingyi Wen[1,2], Fei Zou[1,2], Lan Yan[1,2]

[1]Affiliated Cancer Hospital of Nanchang University, Nanchang, China; [2]Department of Radiology, Jiangxi Provincial Cancer Hospital, Nanchang, China; [3]Department of Nuclear Medicine, Jiangxi Provincial Cancer Hospital, Nanchang, China; [4]Department of Radiotherapy for Head and Neck Tumors, Jiangxi Provincial Cancer Hospital, Nanchang, China; [5]Department of Pathology, Jiangxi Provincial Cancer Hospital, Nanchang, China

Contributions: (I) Conception and design: L Liu, D Peng; (II) Administrative support: L Liu; (III) Provision of study materials or patients: L Liu, D Peng, L Hu; (IV) Collection and assembly of data: D Peng, L Hu, Q Zeng, Q Wen, F Zou, L Yan; (V) Data analysis and interpretation: L Liu, D Peng, Z Chen, Z Liu; (VI) Manuscript writing: All authors; (VII) Final approval of manuscript: All authors.

Correspondence to: Lan Liu. Department of Radiology, Affiliated Cancer Hospital of Nanchang University, Jiangxi Provincial Cancer Hospital, Nanchang 330029, China. Email: liulan6688@163.com.

Background: Abnormal microangiogenesis and microenvironmental disturbances within the Nasopharyngeal carcinoma (NPC) can exacerbate tumor hypoxia, which may increase radiotherapy resistance and thus lead to poor prognosis in NPC patients. A non-invasive imaging technique, dynamic contrast-enhanced magnetic resonance imaging (DCE-MRI), which can reflect the tumor blood perfusion and angiogenesis status, was used to investigate the relationships of DCE-MRI parameters with hypoxia-inducible factor 1 alpha (HIF-1α) expression and tumor grades in NPC patients.

Methods: 42 treatment-naive patients with pathologically confirmed NPC were enrolled in this analysis. Plain magnetic resonance scans and DCE-MRI scans were performed before treatment, and post-processing was performed to calculate the relative enhancement (RE), maximum relative enhancement (MRE), maximum enhancement (ME), wash-in rate (WIR), wash-out rate (WOR), time to peak (TTP), and area under the curve (AUC). Immunohistochemistry was used to detect HIF-1α expression in electronasopharyngeal fiberoscopic specimens. The clinical grade/stage of NPC was jointly assessed by an experienced radiologist and a radiotherapist. The potential correlations of the DCE-MRI parameters with HIF-1α expression and clinical grades were analyzed. The statistical analysis was performed using SPSS 17.0 software package.

Results: Among DCE-MRI parameters, RE, ME, and MRE were associated with the positive expression of HIF-lα in NPC and could reflect the hypoxic status in the local microenvironment of the cancer foci *in vivo*. RE, ME, and MRE were significantly higher in the positive HIF-1α expression group than in the negative HIF-1α expression group (F=5.281, P=0.027; F=11.923, P=0.001; F=6.228, P=0.017). RE, ME, and MRE were significantly correlated with clinical grade (F=3.646, P=0.021; F=3.204, P=0.034, F=3.050, P=0.040) and T stage (F=6.578, P=0.001; F=3.540, P=0.023; F=4.384, P=0.010). The values of RE, MRE, and ME gradually increased as the clinical grade and T stage increased.

Conclusions: DCE-MRI is a valuable imaging technique for the noninvasive evaluation of hypoxia in NPC, the development of individualized treatment protocols, and the prediction of efficacy.

Keywords: Nasopharyngeal carcinoma (NPC); magnetic resonance imaging (MRI); dynamic contrast-enhanced (DCE); hypoxia-inducible factor 1 alpha (HIF-1α)

Submitted Nov 06, 2020. Accepted for publication Feb 22, 2021.
doi: 10.21037/apm-21-303
View this article at: http://dx.doi.org/10.21037/apm-21-303

Introduction

Nasopharyngeal carcinoma (NPC) is one of the most common malignancies in southern China and Southeast Asia, and its common clinical manifestations include nosebleeds, nasal blockage or stuffiness, blurred or double vision, and enlarged lymph nodes in the neck. At present, radiotherapy or concurrent chemoradiotherapy remains the mainstay of treatment of patients with NPC. NPC is moderately or highly sensitive to radiotherapy in most cases; in some other cases, however, NPC responds poorly to radiotherapy, and the patients may die after tumor metastasis, which imposes a significant physical, mental, and economic burdens on the patients and their families. Tumor hypoxia is one of the main causes of the NPC treatment failure. Hypoxia is closely related to the occurrence, invasion, and metastasis of NPC and can reduce the sensitivity of NPC to various therapies. As targeted killing of hypoxic tumor cells has become a focal point in the treatment of NPC, as a safe, effective, and repeatable non-invasive approach for assessing the hypoxic status of NPC will be particularly important for developing clinical treatment protocols (1). Hypoxia-inducible factor 1 alpha (HIF-1α) is an essential regulator of tumor cell adaptation to hypoxia and regulates the angiogenesis, energy metabolism, invasion/metastasis, and radiotherapy tolerance of tumors. It has been one of the most widely used markers of hypoxia in recent years. Dynamic contrast-enhanced magnetic resonance imaging (DCE-MRI) can reflect angiogenic activity and capillary permeability in NPC tissues with the help of intravascular contrast and rapid acquisition techniques. Here, we investigated the relationships among imaging parameters, pathology, and clinical indicators of NPC to assess the status of tumor hypoxia and angiogenesis, with the aim of providing a basis for the non-invasive pretreatment evaluation of NPC hypoxic status, the development of individualized treatment protocols, and the prediction of outcomes. We present the following article in accordance with the STARD reporting checklist (available at http://dx.doi.org/10.21037/apm-21-303).

Methods

Clinical data

A total of 45 treatment-naive patients with pathologically confirmed NPC admitted to the Department of Head and Neck Cancer Radiotherapy of Jiangxi Provincial Cancer Hospital from April 2018 to December 2019 were consecutive enrolled in this prospective study. The inclusion criteria were as follows: (I) with treatment-naive non-keratinizing NPC that was pathologically confirmed after electronic nasopharyngoscopy; (II) with measurable and evaluable nasopharyngeal lesions on MRI; (III) without other serious diseases; and (IV) with signed informed consent. The exclusion criteria were as follows: (I) being allergic to gadolinium contrast agent used for DCE-MRI; (II) unable to undergo MRI due to claustrophobia or other contraindications to MRI; (III) with artifacts on DCE-MRI images or other reasons for poor image quality; and (IV) pregnant or lactating women. Among these 45 NPC patients, the tumor focus was too small to be detected by nasopharyngeal MRI in 1 case, while 2 other patients were uncooperative and the quality of MRI images were of too poor quality for evaluation. Thus, 42 subjects were included in the final analysis. Another 15 patients with chronic inflammatory lesions in the nasopharynx were selected as the control group.

The study was conducted in accordance with the Declaration of Helsinki (as revised in 2013). The study was approved by the Institute Research Ethic Committee of Jiangxi Provincial Cancer hospital (No.: 2018ky022) and informed consent was taken from all individual participants.

MRI and post-processing

All patients were imaged on a superconducting 3.0 T system (Intera 3.0T; Philips Medical Systems, Best, The Netherlands). The patients were asked to lie in the prone position. A Philips 16-channel phased-array head and neck coil (Amsterdam, The Netherlands) was used. Images for transverse scans were acquired with the following

parameters: spin echo (SE) sequence T1-weighted image (T1WI): TR =580 ms, TE =18 ms; turbo spin echo (TSE) sequence T2WI: TR =2,500 ms, TE =90 ms; SE echo-planar imaging (SE-EPI) sequence diffusion-weighted imaging (DWI): TR =5,400 ms, TE =70 ms (with b values of 0 and 1,000 s/mm^{2,} respectively). Meanwhile, images for coronal and sagittal scans were acquired with the following parameters: TSE sequence on coronal T2WI with lipid suppression: TR =2,750 ms, TE =60 ms; SE sequence on sagittal T1WI: TR =600 ms, TE =20 ms. The slice thickness was 5 mm and the interslice distance was 1 mm.

With the use of a high-pressure syringe, 0.1 mmol/kg of MR contrast agent, gadopentetate glucosamine (Gd-DTPA), was injected via the elbow vein at a rate of 3 mL/s; after the injection, the tube was flushed with 15 mL of saline at a rate of 3 mL/s. Fast low-angle shot (FLASH) sequence was used to initiate a multi-phase DCE scan of the nasopharynx [TR =4 ms, TE =2 ms, field of view (FOV) =260×190×90, matrix = 256×256, number of slices =2]; the total time spent was 432 s over 12 phases. The slice thickness was 3 mm and the interslice distance was 0 mm.

The raw DCE-MRI data were transferred to the IntelliSpace Portal (Philips) for post-processing. The largest tumor layer on the contrast-enhanced nasopharyngeal image that could be used to guide the nasopharyngoscopy biopsy was selected, and the region of interest (ROI) was outlined along the tumor edges with the transaxial T2WI lipid suppression sequence and the transaxial DWI sequence as references. During the drawing of ROIs, structures such as the bones, nasopharyngeal cavity, large blood vessels, and muscles should be avoided as possible. For evenly enhanced lesions, the whole lesion was selected as the ROI if possible; for lesions with uneven enhancement, the most obviously enhanced area was selected as the ROI, with the cystic necrosis areas being avoided. The time-signal intensity curve (TIC) was plotted using the T1-perfusion post-processing software package on the IntelliSpace Portal. These TIC curves were divided into three types according to the literature: type I (inflow type), type II (plateau type), and type III (outflow type). Parameters including relative enhancement (RE), maximum relative enhancement (MRE), maximum enhancement (ME), wash-in rate (WIR), wash-out rate (WOR), time to peak (TTP), and area under the curve (AUC) were calculated, among which MRE was calculated using the following formula: MRE = (signal intensity at peak – signal intensity of pre-enhancement)/signal intensity of pre-enhancement × 100%. The measurement data are presented as $\bar{x}$±SD.

Clinical grading and staging of NPC

The clinical stage of NPC was jointly assessed by an experienced radiologist and a radiotherapist in accordance with the American Joint Committee on Cancer (AJCC) Cancer Staging Manual Eighth Edition. T staging and N staging were based on MRI findings of the nasopharynx and neck, while M staging was based on the findings on chest computed tomography (CT), abdominal CT or ultrasound, cranial MRI, whole-body bone scan, and/or positron emission tomography-CT. T stages included the following classifications: Tx = the primary tumor cannot be assessed; T0, no evidence of primary tumor but with cervical lymph node metastasis and positive Epstein–Barr virus infection; T1 = tumor invasion limited to the nasopharyngeal cavity or only affecting the oropharynx or nasal cavity, with no invasion of the parapharyngeal space; T2 = tumor invasion of parapharyngeal space or the adjacent soft tissues such as the inner pterygoid muscle, the outer pterygoid muscle, and the prevertebral muscle; T3 = tumor invasion of the skull base, cervical spine, pterygoid structure, and/or sinus; T4 = tumor invasion of the brain, cranial nerves, hypopharynx, orbit, and parotid gland, along with extensive soft tissue invasion outside the lateral side of the pterygoid muscle. N stages included the following classifications: N_X = regional lymph nodes cannot be assessed; N_0 = no regional lymph node metastasis; N_1 = unilateral cervical lymph node metastasis above the lower edge of the cricoid cartilage, with a maximum diameter of ≤6 cm, or unilateral or bilateral posterior pharyngeal lymph node metastasis, with a maximum diameter of ≤6 cm); N_2 = bilateral cervical lymph node metastasis above the lower edge of the cricoid cartilage, with a maximum diameter of ≤6 cm; N3 = unilateral or bilateral cervical lymph node metastasis with a maximum diameter of >6 cm, and/or metastatic lymph node infiltration below the lower edge of the cricoid cartilage. The M stages included the following classifications: M_0 = without distant metastasis; M_1 = with distant metastasis. The clinical grades included grade 0 (Tis N_0M_0), grade I ($T_1N_0M_0$), grade II ($T_{0-1}N_1M_0$ and $T_2N_{0-1}M_0$), grade III ($T_{0-2}N_2M_0$ and $T_3N_{0-2}M_0$), and grade IV (IVA: $T_4N_{0-2}M_0$ and $T_{0-4}N_3M_0$; IVB: $T_{0-4}N_{0-3}M_1$). The early clinical grades included grades I and II, and the advanced clinical grades were stages III and IV.

Table 1 Clinical features and grades/stages of 42 cases of nasopharyngeal carcinoma

Item	Sex		Age (years)		Clinical grade				T stage				N stage				M stage	
	Males	Females	<58	≥58	I	II	III	IV	T_1	T_2	T_3	T_4	N_0	N_1	N_2	N_3	M_0	M_1
N	29	13	21	21	2	8	18	14	6	11	18	7	12	12	10	8	38	4
Percentage (%)	69	31	50	50	5	19	43	33	14	26	43	17	29	29	24	19	90	10

Pathology and immunohistochemistry

Processing and pathological examination of specimens and detection of HIF-1α with immunohistochemistry

Pathological specimens of NPC were harvested by using electric nasopharyngoscopy. The sections were selected at the sites, and, whenever possible, were corresponded to the ROI outlined during DCE-MRI. The specimens were fixed with 10% formalin solution, embedded in paraffin (hard wax added with some beeswax), and stained with hematoxylin-eosin (HE). The immunohistochemical testing of HIF-1α used the technology of labelled dextran polymer, which the main steps included treatment with an adhesion slide, sectioning of the paraffin-embedded tissue block at 3-μm thickness, baking of slices, dewaxing, washing, high-pressure antigen retrieval, washing, adding of the primary anti-HIF-1α polyclonal antibody, washing, adding of the secondary antibody, counterstaining with hematoxylin, adding of EDTA solution to produce a bright-blue color, gradient alcohol dehydration, xylene treatment, and neutral gum sealing.

Interpretation of the HIF-1α expression with immunohistochemistry

HIF-1α protein was defined as positively stained if the nucleus was brownish yellow in color and had a fine, granular shape, and the staining was regarded as negative if there was no positive reaction. The scoring for the staining intensity was as follows: 0 = no specific staining, 1 = mild staining (light yellow), 2 = moderate staining (brownish yellow), and 3 = strong staining (brown). The proportions of stained cells were also scored; for each sample, 5 fields, with 100 cells/field, were randomly chosen (500 cells in total). The results were interpreted based on the percentage of the positively stained cells among these 50 cells: <5% = negative (scored 0); 5–25% = weakly positive (scored 1), 25–50% = moderately positive (scored 2); >50% = strongly positive (scored 3). The final judgment of HIF-1α protein expression was as follows: total score = staining intensity score + proportion score. The total score was considered negative if it was less than 2 and was considered positive if it was greater than 2.

Statistical analysis

The statistical analysis was performed using the SPSS 17.0 software package (IBM Corp., Armonk, NY, USA). All the values of the DCE-MRI parameters are presented as mean ± standard deviation ($\bar{x}$ ± SD). The count data were analyzed using the χ^2 test or Fisher's exact probability test, the comparisons of the measurement data between two groups were based on *t* test or F test, and the comparisons among multiple groups were based on F test. A P value of <0.05 was considered statistically significant. The diagnostic performance of DCE-MRI parameters for suggesting positive expression of HIF-1α was analyzed using receiver operating characteristic (ROC) curves.

Results

Clinical features and grades/stages of NPC

All 42 patients were pathologically confirmed as non-keratinizing NPC. There were 29 men and 13 women aged 27–76 years (median: 58 years; mean: 53.2±13.6 years). In the control group (n=15), there were 9 males and 6 females aged 30–64 years (median: 48 years; mean: 47.5±10.8 years). The clinical stage of NPC was jointly assessed by an experienced radiologist and a radiotherapist in accordance with the American Joint Committee on Cancer (AJCC) Cancer Staging Manual Eighth Edition. Based on the findings on nasopharyngeal and neck MRI, chest CT, abdominal CT or ultrasound, cranial MRI, whole-body bone scan, and/or PET-CT, the clinical grades were assessed in 42 patients (stage I, n=2; stage II, n=8; stage III, n=18; and stage IV, n=14). Among them, there were 6 patients were in T_1, 11 in T_2, 18 in T_3, and 7 in T_4; 12 in N_0, 12 in N_1, 10 in N_2, and 8 in N_3; and 38 in M_0 and 4 in M_1 (*Table 1*).

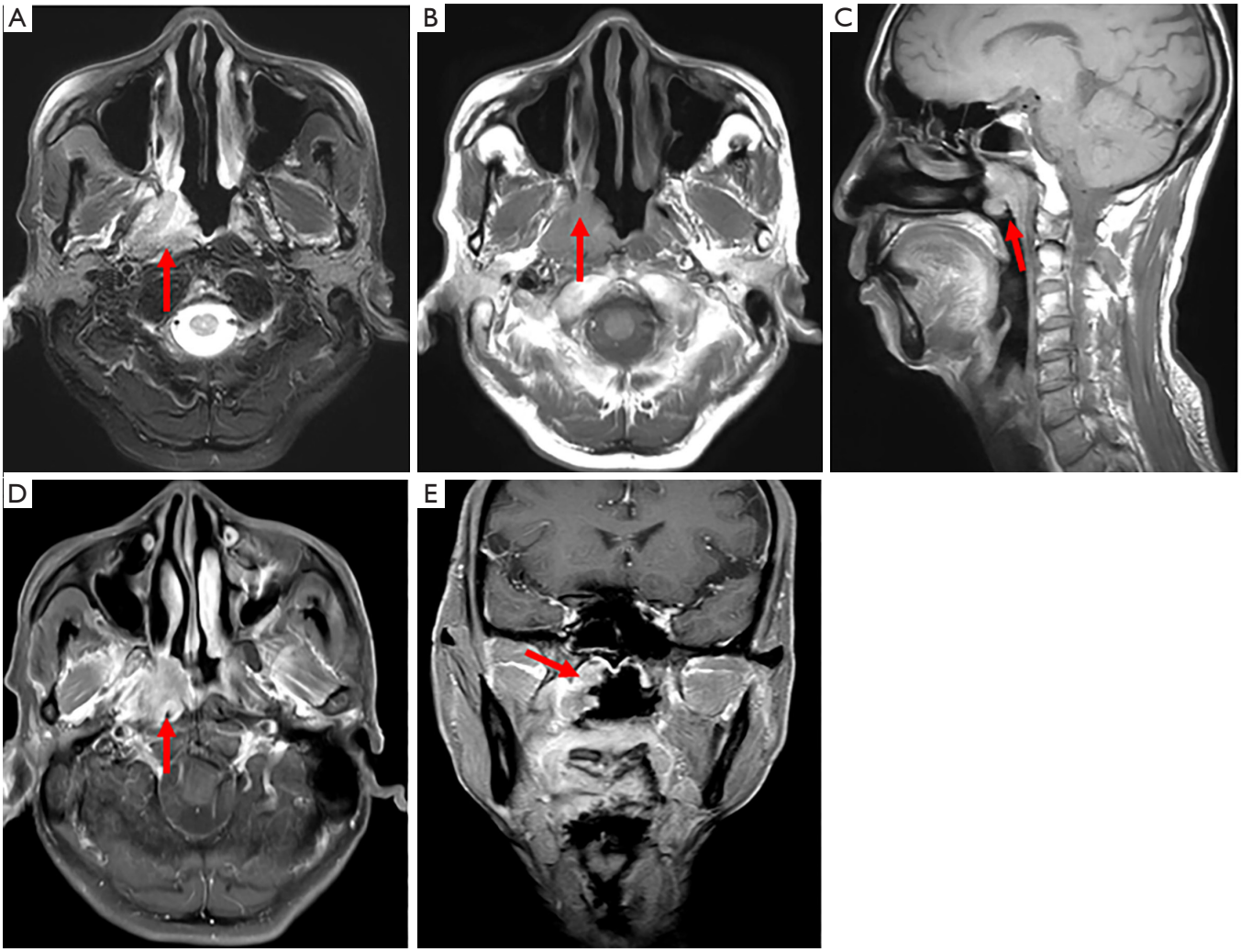

Figure 1 MRI images of nasopharyngeal cancer. Nasopharyngeal carcinoma grade III ($T_3N_1M_0$): the right pharyngeal recess has disappeared, soft tissue masses are visible in the right pharyngeal wall and the posterior parietal wall, the right internal and external pterygoid muscles and the right posterior nostril are invaded, and the skull base bones are damaged. (A) Transaxial T2 with lipid suppression, (B) transaxial T1WI, (C) sagittal T1WI, (D) transaxial contrast-enhanced scan, and (E) coronal-enhanced scans.

DCE-MRI signal characteristics and parameters of NPC

DCE-MRI signal characteristics of NPC

MRI of NPC showed shallowing of the unilateral or bilateral pharyngeal recess, thickening of the nasopharyngeal wall, and formation of irregular soft tissue masses inside the nasopharyngeal cavity (*Figure 1A*,*B*,*C*,*D*,*E*). The nasopharyngeal masses are shown as equal or slightly low signals on T1WI and inhomogeneous, slightly high or high signals on T2WI with fat suppression. Sagittal T1WI and coronal TWI with fat suppression could complement each other with transaxial images, showing tumor invasion in the paranasal sinus cavity, skull base, intracranial regions, cerebral nerves, hypopharynx, orbit, parotid gland, and masticatory muscle as well as cervical lymph node metastasis.

DCE-MRI parameters of NPC

Enhancement and TIC curve of NPC

During the DCE mask, the tumor lesions showed iso-signal intensity to the surrounding muscle tissue; at the early stage of dynamic enhancement, the tumor lesion showed hypertense signals; at the delayed phase on DCE scans, the enhancement of the lesions was slightly weakened. In

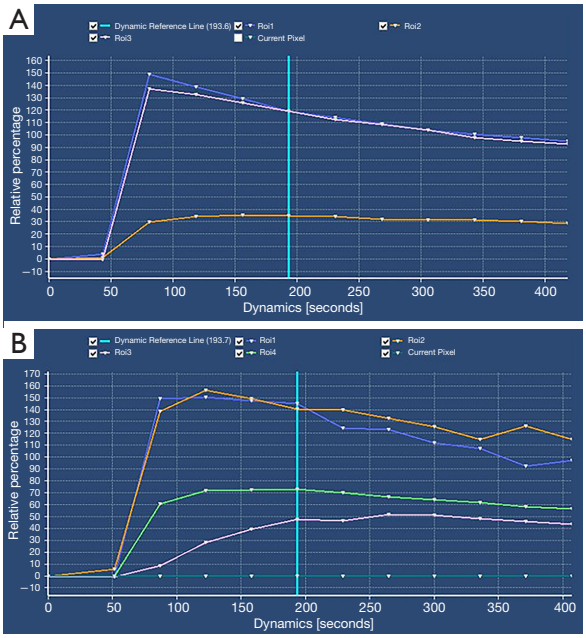

Figure 2 Enhancement and TIC curve of NPC. (A) TIC is a type III curve. In the dynamic enhancement mask, the signals of the cancer focus are similar to those of the muscle tissue; in the early stage of dynamic enhancement, the cancer focus is obviously enhanced with high signals, and there is a rapid and steep ascending period, which reaches a peak at 30 s and then enters a slow-down period. (B) TIC is a type II curve. In the dynamic enhancement mask, the signals of the cancer focus are similar to those of the muscle tissue; in the early stage of dynamic enhancement, the cancer focus is obviously enhanced with high signals, and there is a rapid and steep ascending period, which reaches a peak at 30 s and then plateaus. TIC, time-signal intensity curve; NPC, nasopharyngeal carcinoma.

our current series, all the TIC curves showed a rapid and steep rising period, peaking at 25–30 s, and then entering a plateauing or slowly decreasing period. The curves were type II in 32 cases and type III in 10 cases (*Figure 2A,B*).

DCE-MRI parameters of NPC

The DCE-MRI parameters of NPC were as follows: RE =128.98%±9.89%; ME =1,244.03±203.77; MRE =136.72%±10.14%; TTP =131.76±54.45 s; WIR =21.72±9.31 s-1; WOR =1.54±0.71 s-1; AUC =292,498.76±144,088.05 (*Table 2*, *Figure 3A,B,C,D,E,F*).

Histopathological diagnosis of NPC and immunohistochemical detection of HIF-1α expression

All 42 patients were pathologically diagnosed as non-keratinizing NPC (*Figure 4A,B,C*), 24 of whom (57.14%) had positive HIF-1α expression (*Figure 5A,B*). In contrast, the expression of HIF-1α was negative in all 15 subjects in the control group (*Figure 6A,B*), resulting in a positive rate of 0; the difference between these two groups was statistically significant (P<0.05).

Relationships of the DCE-MRI parameters with clinical features and clinical grades/stages

None of DCE-MRI parameters were significantly correlated with age or sex in 42 NPC patients (all P>0.05). However, RE, ME, and MRE were significantly correlated with clinical stage (F=3.646, P=0.021; F=3.204, P=0.034, F=3.050, P=0.040) and T stage (F=6.578, P=0.001; F=3.540, P=0.023; F=4.384, P=0.010), and the values of RE, MRE, and ME gradually increased as the clinical grade and T stage rose; RE, ME, and MRE values did not correlate with N stage or M stage (all P>0.05). TTP (s), WIR (s-1), WOR (s-1), and AUC showed no significant correlation with

Table 2 Quantitative DCE-MRI parameters of 42 cases of nasopharyngeal carcinoma

Parameter	N	Minimum value	Maximum value	Mean	Standard deviation	Mean ± standard deviation
RE (%)	42	110.16	147.25	128.9795	9.89179	(128.98±9.89)%
ME	42	548.36	1,584.71	1,244.0312	203.77189	1,244.03±203.77
MRE (%)	42	120.16	160.66	136.7169	10.14035	(136.72±10.14)%
TTP (s)	42	47	294	131.76	54.446	(131.76±54.45) s
WIR (s^{-1})	42	4.98	48.93	21.7188	9.31239	(21.72±9.31) s^{-1}
WOR (s^{-1})	42	0.23	3.16	1.5405	0.70597	(1.54±0.71) s^{-1}
AUC	42	159,102.92	998,038.50	292,498.7581	1.44088E5	292,498.76±144,088.05

DCE-MRI, dynamic contrast-enhanced magnetic resonance imaging; RE, relative enhancement; ME, maximum enhancement; MRE, maximum relative enhancement; TTP, time to peak; WIR, wash-in rate; WOR, wash-out rate; AUC, area under the curve.

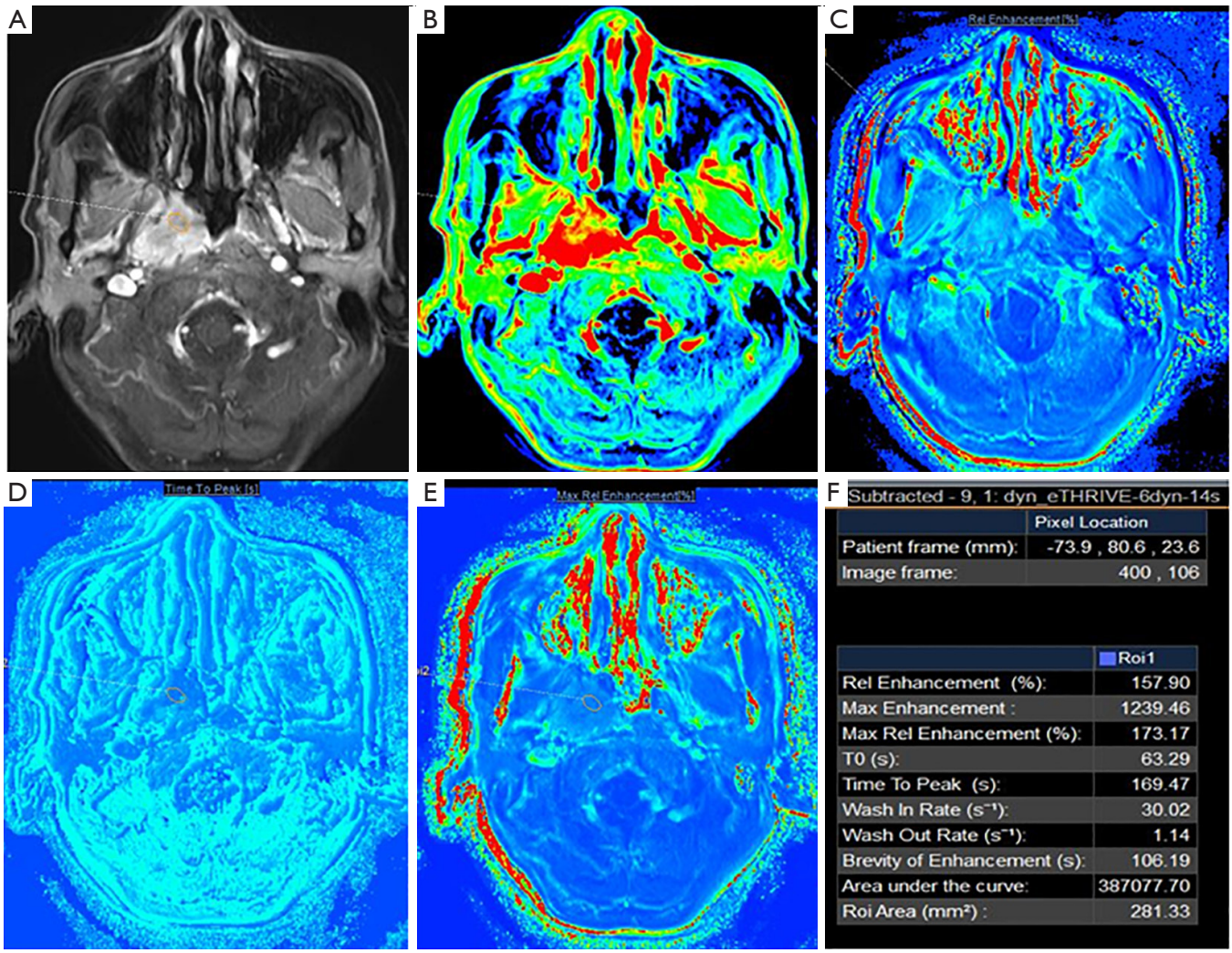

Figure 3 Pseudo-color maps of DCE-MRI parameters of nasopharyngeal carcinoma and the value of each parameter. (A) Nasopharyngeal carcinoma after enhancement, (B) pseudo-color image of AUC, (C) pseudo-color image of RE, (D) pseudo-color image of TTP, (E) pseudo-color image of MRE, (F) value of each parameter. DCE-MRI, dynamic contrast-enhanced magnetic resonance imaging; AUC, area under the curve; RE, relative enhancement; TTP, time to peak; MRE, maximum relative enhancement.

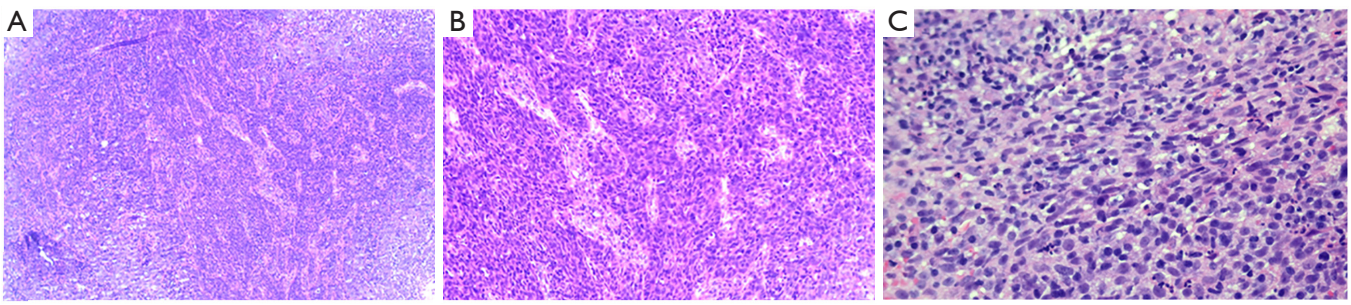

Figure 4 HE staining of non-keratinizing nasopharyngeal carcinoma. (A) The cancer cells are arranged in nests, with lymphocyte interstitium (×100). (B) Atypia occurs in cancer cells, which have large and dark nuclei and mitotic figures (×200). (C) A 400-fold field of view.

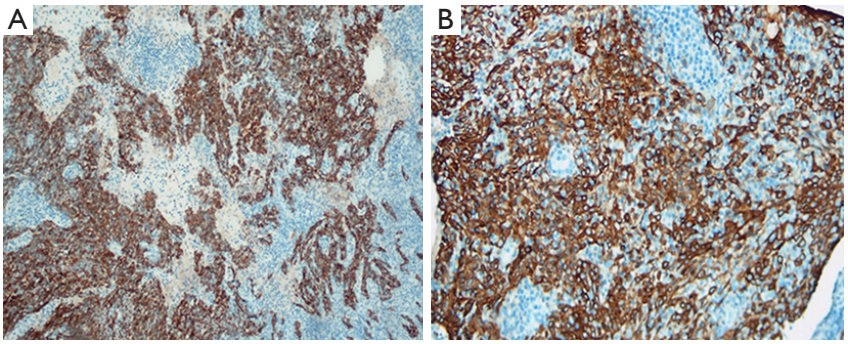

Figure 5 Positive expression of HIF-1a in non-keratinizing nasopharyngeal carcinoma. (A) 100-fold field of view. (B) The cell nuclei are stained as brown-yellow fine particles (400×). HIF-1α, hypoxia-inducible factor 1 alpha.

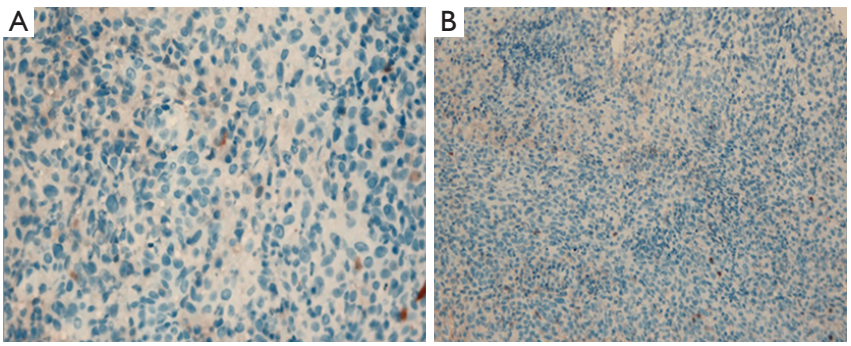

Figure 6 Negative expression of HIF-1a in chronic nasopharyngeal inflammation. (A) A 400-fold field of view. (B) The cell nuclei are not stained brown (100×). HIF-1α, hypoxia-inducible factor 1 alpha.

clinical grade, T stage, N stage, or M stage (*Table 3*).

Relationships of HIF-1α expression with clinical features and clinical grades/stages

Positive HIF-1α expression showed no statistically significant differences in NPC patients according to sex or age (P>0.05) but was significantly correlated with different T stage or clinical grades (P<0.05). The positive expression rate of HIF-1α increased with the elevated grade/stage of NPC: 16.7 % for T_1 (1/6), 36.4 % for T_2 (4/11), 72.2% (13/18) for T_3, and 85.7% (6/7) for T_4; it was 0% (0/2) for grade I, 12.5% (1/8) for grade II, 55.6% (10/18) for grade III, and 92.9% (13/14) for grade IV. The positive expression rate of HIF-1α was 71.9% (23/32) in patients with advanced NPC (grades III–IV), which was significantly higher than that (10.0%; 1/10) in those with early NPC (grades I–II) (P<0.01) (*Table 4*).

Relationships of DCE-MRI parameters of NPC with HIF-1α expression

Among the DCE-MRI parameters, RE, ME, and MRE were significantly higher in the positive HIF-1α expression group than in the negative HIF-1α expression group (F=5.281, P=0.027; F=11.923, P=0.001; F=6.228, P=0.017), whereas TTP, WIR, WOR, and AUC values showed no significant differences between these two groups (P>0.05) (*Table 5*).

ROC curve analysis showed that RE, ME, and MRE values were effective in discriminating HIF-1α-positive or HIF-1α-negative expression, with an AUC of 0.729, 0.819, and 0.690, respectively (*Figure 7* and *Table 6*). The optimal diagnostic thresholds, sensitivities, and specificities of RE, ME, and MRE for discriminating HIF-1α-positive and HIF-1α-negative expression are shown in *Table 7*.

Table 3 Relationships of the DCE-MRI parameters with clinical features and clinical grade/stage

Item	RE (%)	ME	MRE (%)	TTP (s)	WIR (s^{-1})	WOR (s^{-1})	AUC
Sex							
Males	129.00±10.09	1,223.24±210.78	137.36±11.59	136.32±54.18	21.08±8.28	1.50±0.67	305,945.42±158,352.31
Females	128.92±9.84	1,290.4±186.63	135.30±5.88	121.55±55.82	23.15±11.54	1.63±0.81	262,502.35±104,945.41
F	0.001	0.975	0.362	0.655	0.440	0.272	0.812
P value	0.981	0.329	0.551	0.423	0.511	0.605	0.373
Age (years)							
<58	131.36±11.00	1,272.96±225.77	135.50±11.00	131.95±42.92	23.04±9.48	1.63±0.70	270,797.50±91,079.58
≥58	126.60±8.24	1,215.10±179.99	137.93±9.32	131.56±65.08	20.40±9.18	1.46±0.72	314,200.02±182,417.99
F	2.531	0.843	0.595	0.001	0.840	0.606	0.952
P value	0.119	0.364	0.445	0.982	0.365	0.441	0.335
Tumor grade							
I	124.19±1.50	1,146.11±28.72	131.25±3.87	162.55±94.51	27.355±5.01	1.01±0.07	182,543.605±4,937.07
II	121.57±5.67	1,079.38±234.54	128.96±6.66	129.56±45.76	23.78±11.44	1.96±0.61	393,580.53±256,990.95
III	128.60±10.56	1,261.69±152.19	137.36±10.09	132.57±55.54	18.91±8.96	1.43±0.71	250,107.38±79,640.66
IV	134.38±8.74	1,329.4±211.05	141.10±10.16	127.56±57.73	23.35±8.65	1.52±0.74	304,948.83±104,004.18
F	3.646	3.204	3.050	0.233	1.070	1.504	2.503
P value	0.021	0.034	0.040	0.873	0.373	0.229	0.074
T stage							
1	121.83±6.86	1,106.83±35.61	127.27±5.01	136.06±47.67	21.13±6.23	1.48±0.56	266,772.46±85,860.94
2	122.18±4.86	1,144.52±235.78	133.35±9.29	115.96±52.45	20.13±11.49	1.62±0.84	312,694.89±239,949.7
3	133.52±9.69	1,327.42±186.42	139.4±8.67	148.25±55.51	22.16±9.18	1.42±0.66	274,677.12±91,709.61
4	134.13±9.77	1,303.57±171.99	143.21±12.02	110.47±56.81	23.59±9.57	1.78±0.78	328,640.16±109,770.67
F	6.578	3.540	4.384	1.251	0.209	0.504	0.357
P value	0.001	0.023	0.010	0.305	0.889	0.682	0.785
N stage							
0	130.62±8.02	1,230.44±97.70	139.04±9.58	130.2±38.87	26.12±11.1	1.72±0.65	346,178.05±221,189.89
1	126.38±12.39	1,206.63±273.79	133.31±11.59	129.3±58.77	20.39±7.19	1.60±0.55	283,469.39±90,380.18
2	125.18±8.28	1,241.87±168.02	136.69±10.90	132.59±69.30	15.95±7.35	1.30±0.80	228,777.43±76,913.71
3	135.17±7.87	1,323.22±253.44	138.39±7.88	136.72±57.81	24.32±8.48	1.49±0.89	305,175.54±114,953.31
F	2.073	0.537	0.717	0.032	2.782	0.694	1.268
P value	0.120	0.660	0.548	0.992	0.054	0.561	0.299
M stage							
0	128.28±10.01	1,241.82±208.27	136.66±10.61	133.81±51.18	21.35±9.45	1.51±0.68	291,661.02±148,030.91
1	135.58±6.1	1,265.01±178.52	137.26±3.93	112.21±87.43	25.24±8.09	1.87±0.98	300,457.29±115,685.45
t value	2.019	0.046	0.012	0.564	0.625	0.947	0.013
P value	0.163	0.832	0.912	0.457	0.434	0.336	0.909

DCE-MRI, dynamic contrast-enhanced magnetic resonance imaging; RE, relative enhancement; ME, maximum enhancement; MRE, maximum relative enhancement; TTP, time to peak; WIR, wash-in rate; WOR, wash-out rate; AUC, area under the curve.

Table 4 Relationships of HIF-1α expression with clinical features and clinical stage

Item	n	HIF-1α (n, %)		χ^2	P value
		Positive	Negative		
Sex					
Males	29	15 (51.7)	14 (48.3)	1.123	0.289
Females	13	9 (69.2)	4 (30.8)		
Age (years)					
<58	21	15 (71.4)	6 (28.6)	3.500	0.061
≥58	21	9 (42.9)	12 (57.1)		
T stage					
1	6	1 (16.7)	5 (83.3)	–	0.022
2	11	4 (36.4)	7 (63.6)		
3	18	13 (72.2)	5 (27.8)		
4	7	6 (85.7)	1 (14.3)		
N stage					
0	12	5 (41.7)	7 (58.3)	–	0.235
1	12	7 (58.3)	5 (41.7)		
2	10	5 (50.0)	5 (50.0)		
3	8	7 (87.5)	1 (12.5)		
M stage					
0	38	21 (55.3)	17 (44.7)	–	0.623
1	4	3 (75.0)	1 (25.0)		
Tumor grades					
I	2	0 (0.0)	2 (100.0)	–	0.000
II	8	1 (12.5)	7 (87.5)		
III	18	10 (55.6)	8 (44.4)		
IV	14	13 (92.9)	1 (7.1)		
Early grades (I + II)	10	1 (10.0)	9 (90.0)	12.838	0.000
Advanced grades (III + IV)	32	23 (71.9)	9 (28.1)		

*, Fisher exact probability. HIF-1α, hypoxia-inducible factor 1 alpha; ROC, receiver operating characteristic.

Discussion

NPC is one of the more highly prevalent malignant tumors in China, and radiotherapy remains its treatment of choice. At present, MRI is the major imaging technique for the grading/staging and efficacy evaluation of NPC (2). In most cases, NPC responds well to radiotherapy and the prognosis is good. However, the treatment outcomes are poor in some patients, with tumor hypoxia being one of the main reasons for treatment failure. In fact, the presence of hypoxia increases the tolerance of tumors to radiotherapy, leading to poor prognosis (3). It has been found that HIF-1α is highly expressed in malignant tumors such as breast cancer and ovarian cancer, and its expression is significantly correlated with pathological grading, clinical grade, and lymph node metastasis (4-6), suggesting HIF-1α expression is closely involved in the proliferation, invasion, recurrence,

Table 5 Relationships of DCE-MRI parameters of NPC with HIF-1α expression

Item	RE (%)	ME	MRE (%)	TTP (s)	WIR (s^{-1})	WOR(s^{-1})	AUC
HIF-1α							
Positive	131.87±10.84	1,327.58±177.5	139.9±11.21	129.31±51.08	21.58±10.11	1.5±0.68	276,911.22±88,451.92
Negative	125.13±7.03	1,132.63±185.8	132.47±6.68	135.02±59.99	21.9±8.41	1.6±0.76	313,282.14±196,687.8
F	5.281	11.923	6.228	0.110	0.012	0.203	0.650
P value	0.027	0.001	0.017	0.741	0.913	0.654	0.425

DCE-MRI, dynamic contrast-enhanced magnetic resonance imaging; NPC, asopharyngeal carcinoma; HIF-1α, hypoxia-inducible factor 1 alpha; RE, relative enhancement; ME, maximum enhancement; MRE, maximum relative enhancement; TTP, time to peak; WIR, wash-in rate; WOR, wash-out rate; AUC, area under the curve.

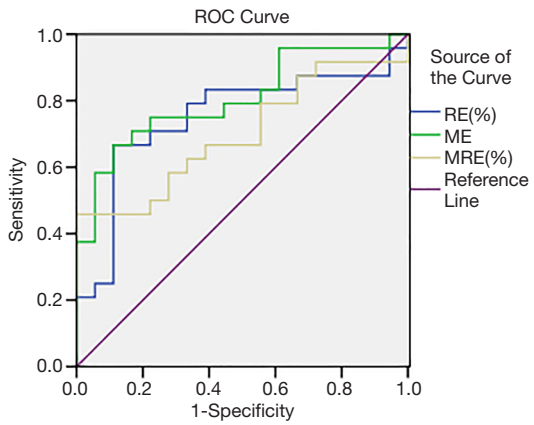

Figure 7 ROC curves of RE, ME, and MRE for distinguishing between positive and negative HIF-1α expressions. ROC, receiver operating characteristic; RE, relative enhancement; ME, maximum enhancement; MRE, maximum relative enhancement; HIF-1α, hypoxia-inducible factor 1 alpha.

and metastasis of malignant tumors. NPC is a vascular-dependent tumor, and abnormal microangiogenesis and microenvironmental disorders within NPC will aggravate tumor hypoxia. In our current study, a non-invasive imaging technique, DCE-MRI, which can reflect the tumor blood perfusion and angiogenesis status, was used to investigate the relationships of DCE-MRI parameters with HIF-1α expression and clinical grade in NPC patients.

Relationships of the HIF- 1α expression with clinical features and clinical grade of NPC

Hypoxic microenvironments can be commonly found in solid tumors, and hypoxia in tumor cells will lead to a series of changes in biological behaviors (7). HIF-1α is a heterodimer that is stably expressed under hypoxic conditions. With a high target gene profile, HIF-1α is involved in regulating tumor growth, proliferation, and angiogenesis. It acts as an important transcription factor regulating downstream elements that affect the energy metabolism, proliferation, and apoptosis of tumor cells, leading to enhanced tumor invasion, progression, and metastasis (8,9).

Sui *et al.* (10) reported positive expression rates of HIF-1α of 79.31% and 10.0% in NPC tissue (n=58) and chronic nasopharyngitis tissue (n=20) respectively, whereas Gong *et al.* (11) found the positive expression rates of HIF-1α to be 51.1% and 0% in NPC tissue (n=92) and chronic nasopharyngitis tissue (n=20), respectively. Thus, the positive expression level of HIF-1α can help to distinguish benign from malignant nasopharyngeal lesions. Similarly, in our current study, the positive rate of HIF-1α was 57.14% (24/42) in NPC patients, which was significantly higher than that (0%, 0/15) in the control group (patients with chronic nasopharyngitis) (P<0.05). Our study further confirmed that HIF-1α was associated with the clinical progression of NPC, suggesting that in NPC (as in many other malignant tumors), tumor cells grow faster than blood vessel formation; thus, when the blood supply cannot meet the demand of tumor cell growth, a hypoxic environment will be formed, which induces HIF-1α expression.

Factors such as the invasion of extra-nasopharyngeal cavity, cranial nerves, and bone, along with regional lymph node and distant metastasis are widely recognized as important biological prognostic indicators of NPC recurrence and metastasis. We assumed that the combined use of the tumor grading/staging-related imaging findings and the immunohistochemical results of HIF-1α expression would allow for a more precise prognostic prediction.

Table 6 ROC curves of RE, ME, and MRE for distinguishing between positive and negative HIF-1α expressions

Outcome variable	Area	Standard error	Asymptotic Sig.	Asymptotic 95% confidence interval	
				Lower limit	Upper limit
RE (%)	0.729	0.082	0.012	0.569	0.889
ME	0.819	0.065	0.000	0.693	0.946
MRE (%)	0.690	0.081	0.037	0.530	0.849

ROC, receiver operating characteristic; RE, relative enhancement; ME, maximum enhancement; MRE, maximum relative enhancement; HIF-1α, hypoxia-inducible factor 1 alpha.

Table 7 Diagnostic performance of RE, ME, and MRE for distinguishing between positive and negative HIF-1α expressions

Parameters	Area under ROC curve	Optimal threshold	Sensitivity	Specificity	Youden index
RE (%)	0.729	128.85	66.7%	88.9%	0.556
ME	0.819	1,284.7	70.8%	83.3%	0.542
MRE (%)	0.690	145.14	37.5%	100.0%	0.375

RE, relative enhancement; ME, maximum enhancement; MRE, maximum relative enhancement; HIF-1α, hypoxia-inducible factor 1 alpha; ROC, receiver operating characteristic.

According to the AJCC Eighth Edition criteria, we determined the T stages (T_1–T_4) of 42 NPC patients based on the extent of invasion shown by MRI. It was found that the tumors gradually infiltrated and grew into the parapharyngeal space, skull base bone, paranasal sinuses, cavernous sinus, and intracranial regions. The positive expression rate of HIF-1α increased with the increase of T stage. The difference of the HIF-1α-positive expression rate among the different T stage groups was statistically significant: 16.7 % for T_1, 36.4 % for T_2, 72.2 % for T_3, and 85.7 % for T_4. The clinical grade of NPC was more significantly correlated with the HIF-1α-positive expression rate: the HIF-1α–positive expression rate was 0% for grade I, 12.5% for grade II, 55.6% for grade III, and 92.9% for grade IV; the HIF-1α-positive expression rate was significantly lower in patients with early NPC (grades I–II) than in patients with advanced NPC (grades III–IV) ($P<0.01$). Thus, there is a correlation between HIF-1α expression and tumor grade/stage; specifically, the hypoxia of cancer tissues is more severe in more advanced tumors, which is more likely to cause HIF-lα expression. As a marker of hypoxia, HIF-lα can reflect the hypoxic status in NPC tissue. It has also been demonstrated that HIF-1α can induce the expression of downstream target genes including vascular endothelial growth factor (VEGF), erythropoietin (EPO), and lactate dehydrogenase (LDHA) (12,13), which allows the continuous differentiation of cells under hypoxia. Tumor cells with a higher grade and/or malignancy adapt to the hypoxic environment, and the conditions for cell proliferation are maintained. New blood vessels are formed at the local areas of the tumor to nourish the cancer cells, maintaining the survival of tumor cells under hypoxia. These newly formed blood vessels will in turn transport malignant cells to various tissues and organs in the body with the help of systemic circulation, thus playing a key role in distant metastasis. Therefore, the development and progression of NPC depend highly on HIF-lα. High HIF-lα expression correlates with clinical grades: HIF-lα is positive in the vast majority of patients with advanced NPC. In fact, these patients are more likely to experience tumor invasion, progression, and metastasis. Therefore, HIF-lα can be used as one of the predictors of poor prognosis in NPC patients.

We found that there was no significant correlation between HIF-lα expression and tumor N stage in NPC, which was consistent with the findings of Huang *et al.* (14). In contrast, Mo *et al.* (15) examined the relationship between HIF-1α expression and N stage in 97 NPC specimens and concluded that HIF-1α expression was closely related to the cervical lymph node metastasis in NPC patients. This discrepancy may be explained by the relatively small sample size in our current study, and therefore future studies with

larger sample sizes are warranted.

Clinical values of DCE-MRI parameters and their relationships with clinical grade/stage

Delineation of target areas for radiotherapy of NPC relies on the precise display of the lesion(s). MRI of the nasopharynx and neck is currently recognized as the optimal means for revealing the shape and size of NPC, the adjacent soft tissues, the invasion of the skull base bones, and the cervical lymph node metastasis. In fact, it has become the main imaging technique for the clinical grading of NPC. DCE-MRI is one of the most promising techniques in MRI (16), and can be divided into quantitative and semi-quantitative approaches (17). Although the semiquantitative technique does not accurately reflect the changes in intravascular contrast concentration (as the quantitative technique does), it may still be a feasible technique in clinical settings because of its advantages of simple operation, convenient post-processing, and easy acquisition of parameters (18). However, most of related studies have mainly focused on quantitative DCE-MRI techniques, while few studies have examined semiquantitative techniques. Semiquantitative DCE-MRI was applied in our current study. Based on the conventional MR, intravascular contrast injection and a rapid MRI acquisition technique were used, which not only revealed the morphological information of the tumor and could be displayed by conventional MRI, but also provided tumor hemodynamic data, which enabled tumor growth assessment in terms of blood perfusion and microcirculation in NPC.

Gadopentetate monomeglumine is the commonly used contrast agent in DCE-MRI. It is an extracellular contrast agent that can pass freely in the intravascular or extracellular spaces. The contrast agent itself does not produce a signal. The reason why the signal intensity of human tissue changes after enhancement is that the gadolinium-based contrast agent indirectly affects the proton relaxation time. After the intravenous injection of paramagnetic gadolinium-based contrast agent, the contrast agent can rapidly enter blood vessels through blood circulation and diffuse into the extracellular spaces. The local blood flow velocity, vascular permeability, extravascular and extracellular spaces, and microvascular density (MVD) in different tissues can affect the distribution and diffusion of gadolinium-based contrast agent, resulting in different signal intensities after enhancement (19,20). Unlike normal tissues, malignant tumors need to make every effort to increase the number of local blood vessels to meet their own metabolic needs for growth, and most of the new blood vessels are immature blood vessels with incomplete vessel walls. The presence of these abnormal blood vessels in tumors constitutes the basis of research on DCE-MRI. There was no type I curve in our current study, and, of the 42 NPC patients, 32 had type II curve and 10 had type III curve. In the early stage of dynamic enhancement, the NPC lesions were significantly enhanced with high signal intensities in all cases. All the TIC curves showed a rapid and steep rising period, peaking at 25–30 s, and then entering a plateauing or slowly decreasing period. This indicates that the blood vessels in NPC tissues are different from those in normal tissues in terms of hemodynamics and function. Abnormal new vessels are rich inside the tumor. In the early stage of enhancement, the gadolinium-based contrast agent rapidly entered the cancer tissue with the help of distorted and widely anastomosed abnormal blood vessels, which caused the signal intensities in the tumor area to increase rapidly and peak within a short period of time which was reflected in the TIC curve as a straight line with a steep rise to the peak; in the middle and late stages of enhancement, however, the signal intensities in the NPC tissue were mostly stable or decreased slowly. This was a result of the higher density of microvessels in NPC than in normal tissues and the incomplete microvascular walls affecting the extravasation of gadolinium-based contrast agent into the extravascular spaces and thus slowing down the clearance of the contrast agent. This result was consistent with the findings of Meng *et al.* (21).

DCE-MRI parameters can, to a certain extent, indirectly reflect angiogenesis and blood perfusion in tumors (22). RE mainly reflects the RE degree of advanced tumor tissues, which is affected by both the gadolinium-based contrast agent diffused into the inter-tissue spaces and in intravascular spaces. ME mainly reflects the enhancement signals early-stage tumors; i.e., the enhancement of tumor tissue when the intravascular gadolinium-based contrast agent reaches its peak, during which time tumor enhancement is affected by MVD. MRE mainly reflects the RE of the lesion when the tumor tissue enhancement reaches its peak; at this time point the contrast agent in the tumor vessels and the contrast agent in the extravascular spaces reach equilibrium. For NPC tissue, DCE-MRI can provide detailed information of the tumor vessels. After the gadolinium-based contrast agent reaches the tumor arteries, it flows into the capillaries and then penetrates through the vascular walls into the extravascular spaces before it

finally returns to the veins. The rate of contrast agent entering from intravascular to extravascular spaces during the contrast-enhanced scans of malignant tumors, benign lesions, and normal tissues can vary, and the enhancement signal of DCE-MRI can reflect the vascular density, vascular permeability, and degree of contrast agent infiltration into extracellular spaces in different tissues (23). In our current study, the RE, ME, and MRE values were positively correlated with the clinical grade and T stage: as the values of RE, MRE, and ME gradually increased, the clinical grade and T stage increased accordingly, suggesting that the values of RE, ME, and MRE can reflect the tumor grade/stage to some extent. NPC is a vascular-dependent malignant tumor that can easily invade adjacent soft tissues, skull base bone, the cavernous sinus, and other structures. Cervical lymph node metastasis and distant metastases in the liver and lungs are common. Neovascularization plays an important role in the occurrence, invasion, and distant metastasis of NPC. In our current study, we found that the RE, ME, and MRE values, which reflect vascular permeability, blood perfusion, and MVD of tumors, were positively correlated with the grade/stage of NPC, indicating that DCE-MRI parameters can reflect the invasiveness of local cancer foci and are closely related to the pathogenesis and progression of NPC. Similarly, Zheng *et al.* (24) proposed that DCE-MRI could non-invasively assess the prognosis of NPC patients.

Relationships of DCE-MRI parameters with HIF-1α expression in NPC

Lindgren *et al.* performed DCE-MRI on 38 ovarian cancer patients and determined its parameters' relationship to HIF-1α expression in cancer tissue specimens. They found DCE-MRI parameters were closely related to positive HIF-1α expression, and further concluded that DCE-MRI could be important adjunct for determining the hypoxic status of ovarian cancer and could guide tailored treatment of hypoxia in clinical settings (25). Xie *et al.* performed DCE-MRI on 34 treatment-naive glioma patients and compared evaluated its parameters' relationship to HIF-1α expression in stereotactic biopsy specimens, concluding that HIF-1α expression was closely related to glioma grade and that DCE-MRI could non-invasively and accurately assess HIF-1α expression; the DCE-MRI parameters could replace HIF-1α to some extent in clinical applications (26).

Among the dynamic-enhanced DCE-MRI parameters examined in our current study, the RE, ME, and MRE values that reflect vascular permeability, blood perfusion, and MVD of the tumors were significantly higher in the positive HIF-1α expression group than in the negative HIF-1α expression group, and the parameter values were positively correlated with the positive expression of HIF-1α, a well-known hypoxia marker. ROC curve analysis showed that RE, ME, and MRE values had good diagnostic performance in identifying positive and negative HIF-1α expressions, with an AUC of 0.729, 0.819, and 0.690, respectively. RE had a sensitivity of 66.7% and a specificity of 88.9% when its threshold was set at 128.85%; ME had a sensitivity of 70.8% and a specificity of 83.3% when its threshold was set at 1,284.7; and MRE had a sensitivity of 37.5% and a specificity of 100% when its threshold was set at 145.14%.

Limitations

First, the number of cases in this study was relatively small and further study with a larger number of cases is needed to confirm our results. Second, our study only focused on the relationship between DCE-MRI and tumor biological marker HIF-1α. In the next step, we intend to study the relationships between DCE-MRI and various tumor biological markers like the immunohistochemical indexes of microvascular density (MVD), vascular endothelial growth factor (VEGF) and Ki67.

Conclusions

HIF-1α, as an immunohistochemical indicator, is the gold standard for tumor hypoxia assessment. However, it requires biopsy and thus is an invasive test; in addition, it cannot reflect the overall characteristics of the tumor. In contrast, DCE-MRI is a non-invasive and radiation-free technique. It can provide both the anatomical and pathophysiological information of tumors and thus is a highly promising non-invasive examination. The results of our current study demonstrate that DCE-MRI parameters can reflect the hypoxic state of local cancer foci in NPC patients, which brings new insight into refining the targeted treatment of NPC.

Acknowledgments

Funding: Multimodal MRI imaging of nasopharyngeal carcinoma: the assessment of tumor hypoxia statue and correlation with hypoxia-inducible factor 1α expression

(The Project Founded by the Science and Technology Department of Jiangxi Province. ID: 20161BBG70103).

Footnote

Reporting Checklist: The authors have completed the STARD reporting checklist. Available at http://dx.doi.org/10.21037/apm-21-303

Data Sharing Statement: Available at http://dx.doi.org/10.21037/apm-21-303

Conflicts of Interest: All authors have completed the ICMJE uniform disclosure form (available at http://dx.doi.org/10.21037/apm-21-303). The authors have no conflicts of interest to declare.

Ethical Statement: The authors are accountable for all aspects of the work in ensuring that questions related to the accuracy or integrity of any part of the work are appropriately investigated and resolved. The study was conducted in accordance with the Declaration of Helsinki (as revised in 2013). The study was approved by the Institute Research Ethic Committee of Jiangxi Provincial Cancer hospital (No.: 2018ky022) and informed consent was taken from all individual participants.

References

1. Anderson CJ, Ferdani R. Copper-64 radiopharmaceuticals for PET imaging of cancer: advances in preclinical and clinical research. Cancer Biother Radiopharm 2009;24:379-93.
2. Pan J, Xu Y, Qiu S, et al. A comparison between the Chinese 2008 and the 7th edition AJCC staging systems for nasopharyngeal carcinoma. Am J Clin Oncol 2015;38:189-96.
3. Xie W, Liu L, He H, et al. Prognostic value of hypoxia-inducible factor-1 alpha in nasopharyngeal carcinoma: a meta-analysis. Int J Biol Markers 2018. [Epub ahead of print]. doi: 10.1177/1724600818778756.
4. Gruber G, Greiner RH, Hlushchuk R, et al. Hypoxia-inducible factor 1 alpha in high-risk breast cancer: an independent prognostic parameter? Breast Cancer Res 2004;6:R191-8.
5. Osada R, Horiuchi A, Kikuchi N, et al. Expression of hypoxia-inducible factor 1alpha, hypoxia-inducible factor 2alpha, and von Hippel-Lindau protein in epithelial ovarian neoplasms and allelic loss of von Hippel-Lindau gene: nuclear expression of hypoxia-inducible factor 1alpha is an independent prognostic factor in ovarian carcinoma. Hum Pathol 2007;38:1310-20.
6. Miyake K, Yoshizumi T, Imura S, et al. Expression of hypoxia-inducible factor-1alpha, histone deacetylase 1, and metastasis-associated protein 1 in pancreatic carcinoma: correlation with poor prognosis with possible regulation. Pancreas 2008;36:e1-9.
7. Graham K, Unger E. Overcoming tumor hypoxia as a barrier to radiotherapy, chemotherapy and immunotherapy in cancer treatment. Int J Nanomedicine 2018;13:6049-58.
8. Gollapudi K, Galet C, Grogan T, et al. Association between tumor-associated macrophage infiltration, high grade prostate cancer, and biochemical recurrence after radical prostatectomy. Am J Cancer Res 2013;3:523-9.
9. Shigeoka M, Urakawa N, Nakamura T, et al. Tumor associated macrophage expressing CD204 is associated with tumor aggressiveness of esophageal squamous cell carcinoma. Cancer Sci 2013;104:1112-9.
10. Sui J, Wu J, Li X, et al. The expression and significance of hypoxia inducible factor-1alpha and microvessel density in human nasopharyngeal carcinoma. Lin Chung Er Bi Yan Hou Tou Jing Wai Ke Za Zhi 2008;22:269-72.
11. Gong L, Li X, Li Z, et al. Expression and clinical significance of HIF-1α and GLUT-1 in nasopharyngeal carcinoma. China Oncology 2012;22:269-75.
12. Sung WW, Chu YC, Chen PR, et al. Positive regulation of HIF-1A expression by EBV oncoprotein LMP1 in nasopharyngeal carcinoma cells. Cancer Lett 2016;382:21-31.
13. Masoud GN, Li W. HIF-1α pathway: role, regulation and intervention for cancer therapy. Acta Pharm Sin B 2015;5:378-89.
14. Huang B, Wong CS, Whitcher B, et al. Dynamic contrast-enhanced magnetic resonance imaging for characterising nasopharyngeal carcinoma: comparison of semiquantitative and quantitative parameters and correlation with tumour

stage. Eur Radiol 2013;23:1495-502.
15. Mo L, Luo Y, Kuang G, et al. The clinical significance of the expression of hypoxia—inducible factor—I alpha in nasopharyngeaI carcinoma. Modern Oncol 2007;15:19-21.
16. Ippolito D, Minutolo O, Cadonici A, et al. Endometrial cancer: diagnostic value of quantitative measurements of microvascular changes with DCE-MR imaging. MAGMA 2014;27:531-8.
17. Zhu J, Xiong Z, Zhang J, et al. Comparison of semi-quantitative and quantitative dynamic contrast-enhanced MRI evaluations of vertebral marrow perfusion in a rat osteoporosis model. BMC Musculoskelet Disord 2017;18:446.
18. Ippolito D, Cadonici A, Bonaffini PA, et al. Semiquantitative perfusion combined with diffusion-weighted MR imaging in pre-operative evaluation of endometrial carcinoma: results in a group of 57 patients. Magn Reson Imaging 2014;32:464-72.
19. Choyke PL, Dwyer AJ, Knopp MV. Functional tumor imaging with dynamic contrast-enhanced magnetic resonance imaging. J Magn Reson Imaging 2003;17:509-20.
20. Koyama T, Tamai K, Togashi K. Staging of carcinoma of the uterine cervix and endometrium. Eur Radiol 2007;17:2009-19.
21. Meng Y, Cheng J, Zhang C. Effect of Dynamic Enhanced MRI in the Assessment of the Prognosis of Patients with Nasopharyngeal Carcinoma. Chinese Journal of CT and MRI 2016;14:1-3.
22. Ippolito D, Minutolo O, Cadonici A, et al. Endometrial cancer: diagnostic value of quantitative measurements of microvascular changes with DCE-MR imaging. MAGMA 2014;27:531-8.
23. Cárdenas-Rodríguez J, Howison CM, Matsunaga TO, et al. A reference agent model for DCE MRI can be used to quantify the relative vascular permeability of two MRI contrast agents. Magn Reson Imaging 2013;31:900-10.
24. Zheng D, Chen Y, Chen Y, et al. Dynamic contrast-enhanced MRI of nasopharyngeal carcinoma: a preliminary study of the correlations between quantitative parameters and clinical stage. J Magn Reson Imaging 2014;39:940-8.
25. Lindgren A, Anttila M, Rautiainen S, et al. Dynamic contrast-enhanced perfusion parameters in ovarian cancer: Good accuracy in identifying high HIF-1α expression. PLoS One 2019;14:e0221340.
26. Xie Q, Wu J, Du Z, et al. DCE-MRI in Human Gliomas: A Surrogate for Assessment of Invasive Hypoxia Marker HIF-1A Based on MRI-Neuronavigation Stereotactic Biopsies. Acad Radiol 2019;26:179-87.

(English Language Editor: J. Gray)

Cite this article as: Liu L, Hu L, Zeng Q, Peng D, Chen Z, Huang C, Liu Z, Wen Q, Zou F, Yan L. Dynamic contrast-enhanced MRI of nasopharyngeal carcinoma: correlation of quantitative dynamic contrast-enhanced magnetic resonance imaging (DCE-MRI) parameters with hypoxia-inducible factor 1α expression and tumor grade/stage. Ann Palliat Med 2021;10(2):2238-2253. doi: 10.21037/apm-21-303

